British Journal of Clinical Pharmacology

Br J Clin Pharmacol (2016) 81 1153–1164 1153

DRUG METABOLISM

Scaling factors for the *in vitro–in vivo* extrapolation (IV–IVE) of renal drug and xenobiotic glucuronidation clearance

Correspondence Emeritus Professor Kathleen M. Knights, PhD, Department of Clinical Pharmacology, School of Medicine, Flinders University, Adelaide, South Australia, Australia, 5001. Tel.: +61 8 8204 4331; Fax: +61 8 8204 5114. E-mail: kathie.knights@flinders.edu.au

Received 4 November 2015; **revised** 19 January 2016; **accepted** 21 January 2016

Kathleen M. Knights[1], Shane M. Spencer[1], John K. Fallon[2], Nuy Chau[1], Philip C. Smith[2] and John O. Miners[1]

[1]*Department of Clinical Pharmacology and Flinders Centre for Innovation in Cancer, School of Medicine, Flinders University, Adelaide, South Australia, Australia, 5001 and* [2]*Division of Molecular Pharmaceutics, Eshelman School of Pharmacy, University of North Carolina at Chapel Hill, Chapel Hill, North Carolina 27599, USA*

Keywords human kidney microsomes, microsomal yield, renal drug glucuronidation clearance, UGT1A9, UGT2B7

AIM

To determine the scaling factors required for inclusion of renal drug glucuronidation clearance in the prediction of total clearance via glucuronidation (CL_{UGT}).

METHODS

Microsomal protein per gram of kidney (MPPGK) was determined for human 'mixed' kidney ($n = 5$) microsomes (MKM). The glucuronidation activities of deferiprone (DEF), propofol (PRO) and zidovudine (AZT) by MKM and paired cortical (KCM) and medullary (KMM) microsomes were measured, along with the UGT 1A6, 1A9 and 2B7 protein contents of each enzyme source. Unbound intrinsic clearances ($CL_{int,u,UGT}$) for PRO and morphine (MOR; 3- and 6-) glucuronidation by MKM, human liver microsomes (HLM) and recombinant UGT1A9 and 2B7 were additionally determined. Data were scaled using *in vitro–in vivo* extrapolation (IV–IVE) approaches to assess the influence of renal $CL_{int,u,UGT}$ on the prediction accuracy of the calculated CL_{UGT} values of PRO and MOR.

RESULTS

MPPGK was 9.3 ± 2.0 mg g^{-1} (mean ± SD). The respective rates of DEF (UGT1A6), PRO (UGT1A9) and AZT (UGT2B7) glucuronidation by KCM were 1.4-, 5.2- and 10.5-fold higher than those for KMM. UGT 1A6, 1A9 and 2B7 were the only enzymes expressed in kidney. Consistent with the activity data, the abundance of each of these enzymes was greater in KCM than in KMM. The abundance of UGT1A9 in MKM (61.3 pmol mg^{-1}) was 2.7 fold higher than that reported for HLM.

CONCLUSIONS

Scaled renal PRO glucuronidation $CL_{int,u,UGT}$ was double that of liver. Renal $CL_{int,u,UGT}$ should be accounted for in the IV–IVE of UGT1A9 and considered for UGT1A6 and 2B7 substrates.

WHAT IS ALREADY KNOWN ABOUT THIS SUBJECT

- Multiple drugs, non-drug xenobiotics and endobiotics are glucuronidated by human kidney.
- UDP-glucuronosyltransferase (UGT) 1A proteins and UGT2B7 are variably expressed in the tubule components of the human nephron.

DOI:10.1111/bcp.12889

- Development of kidney specific *in vitro–in vivo* extrapolation (IV–IVE) approaches is hampered by the limited availability of microsomal protein per gram of kidney (MPPGK) and knowledge of the content and anatomic distribution of individual UGT enzymes.

WHAT THIS STUDY ADDS

- This study provides scaling factors to assess the relative contribution of the kidney to renal drug clearance via glucuronidation.
- It demonstrates anatomic differences in renal glucuronidation activity and provides data on the contents of UGT1A6, UGT1A9 and UGT2B7 in human kidney cortex and medulla.
- It establishes that UGT1A9 is 2.7-fold more abundant in human kidney microsomes than hepatic microsomes, indicating the need to include renal glucuronidation unbound intrinsic clearance in IV–IVE predictions for substrates glucuronidated by UGT1A9.

Introduction

The human kidney has an array of functions that include the regulation of blood osmolarity, volume, ionic composition and pH, the production of renin, 1,25-dihydroxyvitamin D, erythropoietin, prostaglandins and bradykinin, and the excretion of endogenous metabolites and xenobiotics. The cortex is characterized by the presence of glomeruli, tufts of capillaries and numerous convoluted epithelial structures that form the renal tubules. In contrast, the medulla consists only of tubules and renal blood vessels. A previous study from this laboratory identified that UDP-glucuronosyltransferase (UGT) 1A proteins and UGT2B7 are variably expressed throughout the tubule components of the human nephron [1]. The greatest expression of UGT1A proteins occurred in the cortical proximal convoluted tubules, while variable and lower expression of UGT2B7 was observed in both cortical and medullary tubules. Consistent with a high to low gradient of UGT1A and UGT2B7 expression from the outer cortex through to the inner medulla, we further demonstrated that the intrinsic clearance for S-naproxen glucuronidation, which is catalyzed predominantly by UGT2B7 (with lesser contributions from UGT 1A6 and 1A9 [2]), was 4.5-fold higher in kidney cortical microsomes (KCM) compared with kidney medullary microsomes (KMM) [1]. Other reports have similarly demonstrated lower glucuronidation activity in renal medulla [3–5].

Multiple drugs, non-drug xenobiotics and endobiotics, including paracetamol, carbamazepine, codeine, dapagliflozin [6], fatty acids, furosemide, gemfibrozil, ibuprofen, ketoprofen, leukotrienes, mefenamic acid, mycophenolic acid, naloxone, naproxen, prostaglandins, propofol (PRO), retigabine and valproic acid have been shown to be glucuronidated by whole human kidney microsomes [[7, 8] and references therein]. Indeed, specific activities for the glucuronidation of several drugs (e.g. dapagliflozin, mycophenolic acid and PRO) by kidney exceeds that of liver [6, 9–11], and there are *in vivo* data suggesting that renal metabolism contributes significantly to PRO clearance [12]. Despite these observations, reliable kidney-specific *in vitro–in vivo* extrapolation (IV–IVE) models are not yet available and inclusion of renal glucuronidation data in IV–IVE studies has been limited [9, 13–15]. In particular, the development of kidney-specific IV–IVE models has been hampered by limited data of microsomal protein per gram of kidney (MPPGK) [13, 14] and knowledge of the abundance and anatomic distribution of individual renal UGT enzymes. Both are essential for generating the scaling factors required to convert *in vitro* enzyme kinetic data to an *in vivo* drug clearance via glucuronidation [16].

Quantitative RT-PCR is used to determine UGT mRNA expression [17, 18] while quantification of UGT protein content has recently utilized isotopically labelled peptides and nano-UPLC-MS/MS analyses [19–22]. The latter studies have principally used human liver microsomes (HLM). By contrast, data from human kidney are limited to reports of one to two individuals, the use of pooled kidney microsomes or kidney homogenate [19, 23, 24].

In this study we report MPPGK using five human kidneys and the results of comparative studies of UGT enzyme activity coupled with UGT protein quantification using mixed (whole) kidney microsomes (MKM), KCM, KMM and recombinant human UGT1A9 and UGT2B7. For the first time we provide data on the anatomic distribution and content of UGT 1A6, 1A9 and 2B7, identify the applicability of MKM for *in vitro* studies and show significant correlations between renal UGT enzyme content and activity. Additionally, unbound intrinsic glucuronidation clearances ($CL_{int,u,UGT}$) were determined for PRO and morphine (MOR) 3- and 6-glucuronidation using MKM, human liver microsomes (HLM) and UGT1A9 and UGT2B7. These data were then scaled to assess the impact of renal $CL_{int,u,UGT}$ on the prediction of IV–IVE for total CL via glucuronidation for PRO and MOR.

Methods

Materials

Alamethicin (from *Trichoderma viride*) was purchased from A. G. Scientific (San Diego, CA, USA). Zidovudine (AZT), AZT-glucuronide, β-estradiol (β-E2), β-estradiol-3-D-glucuronide, MOR 3-glucuronide (MOR(3-G)), PRO, testosterone (TST), TST-17-glucuronide and trifluoperazine (TFP) from Sigma-Aldrich (Sydney, Australia), deferiprone-3-*O*-glucuronide and PRO glucuronide from Toronto Research Chemicals (Toronto, ON, Canada), MOR from GlaxoSmithKline (Melbourne, Australia) and MOR 6-glucuronide (MOR(6-G)) from Salford Ultrafine Chemicals (Manchester, UK). Deferiprone (DEF) was provided by Dr John Connelly (Apopharma Inc., Toronto, ON, Canada). For UGT protein quantification, stable isotope labelled (SIL) proteotypic peptides in aqueous solution (1 nmol 200 μl^{-1}) containing 5 or

20% acetonitrile were purchased from Thermo Biopolymers (Ulm, Germany; Material No. HPA97QP010, >97% purity). Ammonium bicarbonate, formic acid, acetic acid, iodoacetamide, dithiothreitol and β-casein were purchased from Sigma-Aldrich (St Louis, MO, USA), acetonitrile (HPLC grade) from Fisher Scientific (Pittsburg, PA, USA) and trypsin Gold mass spectrometry grade from Promega (Madison, WI, USA). Pooled HLM (150 donor pool; equal number of male and female donors) and UGT1A9 (batch 2 228 592) and UGT2B7 (batch 38 943) Supersomes™ were provided by Corning Gentest (Palo Alto, CA, USA). All other reagents and solvents used were of the highest analytical grade available.

Human kidney tissue and kidney microsomes

Kidney tissue from Caucasians undergoing radical nephrectomy for malignant disease was provided by the joint Flinders Medical Centre/Repatriation General Hospital Tissue Bank (Adelaide, South Australia). Approval for the collection and use of human kidney tissue for *in vitro* studies was obtained from the Southern Adelaide Clinical Human Research Ethics Committee. All tissue used was distant from the primary tumour and was reported by a specialist histopathologist to be histologically normal for the age of the donors (43–79 years), with only benign nephrosclerosis and hypertensive-like vascular changes observed. Whole kidney (mixed cortical/medullary) tissue was available from two females (K12-K13) and three males (K14-K16). Paired cortical and medullary tissue (both obtained from the same kidney) was available from five males (K2, K7, K9-K11, for details of individual subjects refer to Supporting Information Table S1).

Mixed kidney microsomes (MKM, n = 5), kidney cortical microsomes (KCM, n = 5) and kidney medullary microsomes (KMM, n = 5) were prepared by differential ultracentrifugation as detailed by Tsoutsikos *et al*. [25]. Microsomal protein was resuspended either in Na_2HPO_4, pH 7.4 containing 20% (w/v) glycerol (for UGT activity assays) or buffer only for UGT protein quantification. MKM, KCM and KMM pools were prepared by combining equal protein amounts of microsomes from the relevant kidneys. Total protein concentration was measured [26] and all samples stored at −80°C until used.

Determination of microsomal protein g^{-1} of kidney (MPPGK)

Correction factors for the loss of kidney microsomal protein during preparation of MKM (K12-K16) were determined by measurement of NADPH cytochrome c reductase activity. Briefly, either homogenate or microsomal protein (0.1 mg ml^{-1}) was added to a solution (2.2 ml) containing cytochrome c (5 μM), potassium cyanide (300 μM) and 0.1 M phosphate buffer (pH 6.8) and preincubated (5 min, 37°C). Samples (1 ml) were transferred to two quartz cuvettes. Water (10 μl) was added to the reference cuvette and NADPH (10 mM, 10 μl) added to the sample cuvette. Absorbance was monitored at 550 nm and NADPH cytochrome c reductase activity calculated using an extinction coefficient of 27.7 cm^{-1} mM^{-1} [27, 28]. The recovery of microsomal protein, and hence fraction of microsomal protein loss during preparation, was determined as (equation (1)):

$$\text{Recovery factor} = \frac{\text{microsomal cytochrome c reductase (nmol per tissue sample)}}{\text{homogenate cytochrome c reductase (nmol per tissue sample)}} \quad (1)$$

Values of MPPGK corrected for microsomal protein loss during preparation were determined using equation (2) [29]:

$$\text{MPPGK}\ (\text{mg g}^{-1}) = \frac{\text{specific activity homogenate}\ (\text{nmol cyt c reduced min}^{-1}\text{mg}^{-1}) \times (\text{mg homogenate protein g}^{-1}\ \text{kidney})}{\text{specific activity microsomes}\ (\text{nmol cyt c reduced min}^{-1}\text{mg}^{-1})} \quad (2)$$

Human kidney microsomal UGT activities

Kidney microsomal UGT 1A1, 1A4, 1A6, 1A9, 2B7 and 2B15/17 activities were determined using β-E2, TFP, DEF, PRO, AZT and TST as the respective enzyme selective substrates [30]. For all activity studies the probe substrate concentrations were four to five times the approximate K_m or S_{50} for each compound: β-E2 50 μM (S_{50} 10 μM, [31]), DEF 20 mM (K_m 4 mM, [32]), PRO 500 μM (K_m 125 μM, [33]), AZT 5 mM (K_m 1 mM, [34]) and TST 30 μM (K_m 6 μM, [35]). However, due to the substrate inhibition observed with TFP glucuronidation, experiments were performed at the substrate K_m (60 μM, [36]). Activity assays were performed in triplicate with MKM (n = 5), KCM (n = 5) and KMM (n = 4). Insufficient KMM was available for K11 for activity studies. HLM were used as the positive control in all activity studies. Microsomal protein concentrations, incubation components, duration of incubation, reaction termination procedure and quantification of β-E2, DEF, PRO, AZT, TST and TFP glucuronides by HPLC were as described in previous publications from this laboratory [31–36]. Overall within-day reproducibilities were determined for each assay by measuring glucuronide formation in 8–10 separate incubations of the

same batch of pooled HLM at three substrate concentrations (low, mid, high) that spanned the ranges used to characterize enzyme kinetic parameters. Coefficients of variation ranged from 1.8% to 6.9%. The lower limits of quantification assessed as three times background noise, ranged from 0.002 to 0.005 μM, which corresponds to rates of glucuronide formation of <0.5 pmol min^{-1} mg^{-1}.

PRO glucuronidation and MOR 3- and 6-glucuronidation kinetics by HLM, MKM and recombinant UGT1A9 and UGT2B7

The kinetics of PRO (10 – 300 μM) glucuronidation and MOR (100 – 3000 μM) 3- and 6-glucuronidation by pooled HLM and pooled MKM in the presence of 2% (w/v) BSA and recombinant UGT1A9 and UGT2B7 (Supersomes) were determined according to Rowland *et al*. [33] and Uchaipichat *et al*. [37], respectively. The protein concentration of MKM and HLM present in incubations was 0.5 mg ml^{-1}, while the protein concentration of UGT1A9 and UGT2B7 Supersomes in incubations was 0.25 mg ml^{-1} and 1 mg ml^{-1}, respectively. PRO, but not MOR [38], binds to HLM plus BSA. Thus, the previously determined $f_{u,mic}$ value of 0.20 was used to correct for PRO binding to incubation constituents [33].

Quantification of human kidney microsomal UGTs and recombinant (Supersome) UGT1A9 and UGT2B7

Protein from MKM, KCM and KMM was diluted to 1 mg ml^{-1} with Na_2HPO_4 and stored at −80°C. Samples (1 μg) of recombinant UGT1A9 and UGT2B7 were added to 19 μg of rat liver microsomes (final protein concentration 20 μg per sample). Samples were analyzed using minor modifications of previously published methods [19, 20, 39]. Briefly, microsomal protein (20 μg, 20 μl of 1 mg ml^{-1} suspension) was added to a solution of ammonium bicarbonate (50 μl, 50 mM), β-casein (0.5 μg, 10 μl of 0.05 mg ml^{-1}) and dithiothreitol (10 μl, 40 mM). Following denaturation and reduction at 65°C, samples were carbamidomethylated with iodoacetamide (10 μl, 135 mM). Trypsin (1 μg, 10 μl of 0.1 mg ml^{-1}) was then added to give a microsomal protein to trypsin ratio of 20 : 1 in each sample. Samples were then digested for 4 h at 37°C. Following the addition of acetonitrile to terminate the digestion reaction, a solution (10 μl) containing SIL peptides (1 pmol of each) was added to each sample. Residual acetonitrile was removed in a vacuum before treating with solid phase extraction (Strata-X 33u Polymeric Reversed Phase, 10 mg ml^{-1}, Phenomenex, Torrance, CA, USA). The solid phase extraction eluate was evaporated to dryness under vacuum and reconstituted in 50 μl modified mobile phase A (water/acetonitrile/formic acid 98/2/0.1; i.e. 2% ACN instead of 1%) before analysis by nanobore UPLC-MS/MS (selected/multiple reaction monitoring mode). Mobile phase B was 100% acetonitrile. The chromatographic and mass spectrometric instrumentation and conditions were as described previously [20]. The separation conditions were 100% A at start, reducing to 58% A at 24 min, then 5% A at 24.5 min for 3 min and 100% A at 28 min for 7 min (total run time 35 min). Multiple reaction monitoring (MRM) data were processed using MultiQuant 2.0 (AB SCIEX). Peaks were smoothed prior to integration and area ratios of unlabelled/SIL peptides were determined using the sum of the two MRMs monitored.

Data analyses

All kidney microsomal UGT activities were performed in triplicate and the values averaged to obtain a single value for each individual kidney. The variation between samples was <5%. Data are reported as mean ± SD (n = 5 kidneys). Correlations between UGT protein content in MKM, KCM and KMM and the respective glucuronidation activities and correlations between the microsomal contents of UGT1A6/UGT1A9, UGT1A6/UGT2B7 and UGT1A9/UGT2B7 were assessed using the non-parametric Spearman rank method. A value of $P < 0.05$ was considered statistically significant. PRO and MOR glucuronidation kinetic data were fitted with the Michaelis–Menten equation using EnzFitter (version 2.0; Biosoft, Cambridge, UK).

Unbound intrinsic clearance ($CL_{int,u}$) values for PRO and MOR glucuronidation by MKM and HLM were calculated as V_{max}/K_m and subsequently scaled for microsomal protein yield (mg g^{-1}) and organ weight (g kg^{-1} body weight) to provide a whole organ $CL_{int,u,UGT}$ (ml min^{-1} kg^{-1}). The respective microsomal protein yields (mg g^{-1} tissue) and organ weights (g kg^{-1} body weight) used in calculations were 9.3 mg g^{-1} (see Results section) and 4.5 g kg^{-1} for kidney [15], and 32 mg g^{-1} [16] and 21.4 g kg^{-1} [15] for liver. In the

Table 1

Glucuronidation rates of DEF, PRO and AZT and contents of UGT 1A6, 1A9 and 2B7 using mixed kidney microsomes (MKM). Tabulated data for UGT contents, enzyme activities and normalized enzyme activities represent the mean ± SD (95% CI), n = 5 (K12-K16). UGT enzyme activities of the MKM pool (K12-K16) normalized for UGT content are the means of triplicate determinations

UGT enzyme	UGT content (pmol-UGT mg^{-1})	MKM UGT activity (pmol-G† min^{-1} mg^{-1})	MKM Normalized UGT activity (pmol-G† min^{-1} pmol-UGT)	MKM pool Normalized UGT activity (pmol-G† min^{-1} pmol-UGT)
1 A6	4.7 ± 1.4 (3.5, 5.9)	21 019 ± 7836 (14 151, 27 887)	4395 ± 639 (3835, 4955)	4008
1 A9	61.3 ± 20.1 (44.3, 78.3)	5656 ± 2191 (3736, 7576)	92 ± 6 (87, 97)	103
2B7	37.6 ± 17.4 (22.3, 52.9)	1229 ± 598 (705, 1753)	33 ± 2 (31, 35)	31

†pmol-G refers to formation of DEF glucuronide (UGT1A6), PRO glucuronide (UGT1A9), or AZT glucuronide (UGT2B7).

absence of a kidney-specific model, the whole organ $CL_{int,u,UGT}$ values were scaled using the well-stirred model to give a predicted total CL via glucuronidation (CL_{UGT}) for both kidney and liver (equation (3)).

$$CL_{UGT} = \frac{Q \; x \; f_{u,b} \; x \; CL_{int,u,UGT}}{Q + \left(f_{u,b} \; x \; CL_{int,u,UGT}\right)} \quad (3)$$

Organ blood flows (Q) were taken as 16.4 ml min^{-1} kg^{-1} for kidney and 20.7 ml min^{-1} kg^{-1} for liver [15]).The fraction of PRO unbound in blood was taken as 0.015 [15], assuming a blood : plasma concentration ratio of 1.0. The fraction of a PRO dose eliminated via glucuronidation was taken as 53% [14], systemic clearance as 108 l h^{-1} and clearance via glucuronidation as 57 l h^{-1} [33].

Mean *in vivo* disposition data for MOR were calculated from values of individual studies reported in the review of Milne et al. [40]: plasma clearance following intravenous administration 86.1 l h^{-1}, percent urinary recoveries of MOR 3- and 6-glucuronides, 55% and 10.2%, respectively, fraction or MOR unbound in plasma, 0.75 and blood/plasma concentration ratio 1.15.

Results

Determination of MPPGK

The average weight of mixed (cortical/medullary) kidney tissue available for preparation of MKM was 0.9 ± 0.2 g. Activities of cytochrome c reductase in the mixed kidney homogenate fractions and matched microsomal fractions were 3.3 ± 0.9 (95% CI 2.5, 4.1) μmol min^{-1} g^{-1} and 19.1 ± 4.8 (95% CI 14.9, 23.3) μmol min^{-1} g^{-1}, respectively. The average percentage of microsomal protein lost during preparation was 33.9 ± 11.8% (95% CI 23.5, 44.3), while the mean MPPGK corrected for loss of microsomal protein was 9.3 ± 2.0 mg g^{-1} (95% CI 7.6, 11).

Mixed kidney microsomal UGT activities

Incubations of pooled MKM did not form the glucuronides of β-E2 (UGT1A1), TFP (UGT1A4) or TST (UGT 2B15/2B17). In contrast, HLM (used as a positive control) catalyzed the glucuronidation of β-E2, TFP and TST with respective mean rates of 348, 350 and 108 pmol min^{-1} mg^{-1}. The mean rates of DEF (UGT1A6), PRO (UGT1A9) and AZT (UGT2B7) glucuronidation by pooled MKM were high, 18 999, 6309 and 1183 pmol min^{-1} mg^{-1}, respectively. Subsequent activity studies using individual MKM from K12-K16 and DEF, PRO and AZT established that the rates of glucuronidation of each probe substrate when expressed as either pmol glucuronide (pmol-G) min^{-1} mg^{-1} microsomal protein or as activity normalized for UGT expression (pmol-G min^{-1} $pmol^{-1}$ UGT), were comparable with the MKM pool (Table 1).

Table 2

Glucuronidation rates of DEF, PRO and AZT and contents of UGT 1 A6, 1 A9 and 2B7 using cortical (KCM) and medullary (KMM) microsomes. Tabulated data for UGT contents, enzyme activities and normalized enzyme activities represent the mean ± SD (95% CI), *n* = 5 (K2, K7, K9-K11). Enzyme activities of the KCM and KMM pools normalized for UGT content are the means of triplicate determinations

UGT enzyme	UGT content (pmol-UGT mg^{-1}) KCM	KMM	Content ratio C : M	UGT activity (pmol-G† min^{-1} mg^{-1}) KCM	KMM	Activity ratio C : M	Normalized UGT activity (pmol-G† min^{-1} $pmol^{-1}$ pmol-UGT) KCM	KMM	Normalized activity ratio C : M	Normalized UGT activity (pmol-G† min^{-1} $pmol^{-1}$ pmol-UGT) KCM pool	KMM pool	Normalized activity ratio (pool) C : M
UGT1A6	3.5 ± 2.1 (1.7, 5.3)	1.6 ± 0.7 (1, 2.2)	2.7 ± 2.2 (0.8, 4.6)	10 503 ± 7389 (4027, 16 979)	5255 ± 2465 (3095, 7415)	1.4 ± 0.4 (1.1, 1.7)	3150 ± 1697 (1663, 4637)	3939 ± 2143 (2061, 5817)	1.0 ± 0.9 (0.2, 1.8)	3506	3986	0.9
UGT1A9	40 ± 19.1 (24, 56)	7.5 ± 2.4 (5, 9)	6.2 ± 4.5 (3.2, 9.2)	5072 ± 2864 (2562, 7582)	905 ± 299 (643, 1167)	5.2 ± 4.1 (1.6, 8.8)	119 ± 25 (98, 140)	105 ± 18 (89, 121)	1.1 ± 0.2 (0.9, 1.3)	124	143	0.9
UGT2B7	24.8 ± 15.2 (12, 38)	4.4 ± 1.8 (2.9, 5.9)	7.2 ± 6.2 (1.8, 12.6)	577 ± 417 (212, 942)	70 ± 27 (47, 93)	10.5 ± 13.8 (-1.5, 22)	22 ± 4 (13, 31)	15 ± 6 (10, 20)	1.8 ± 1.4 (0.6, 3)	15	11	1.4

†pmol-G refers to formation of DEF glucuronide (UGT1A6), PRO glucuronide (UGT1A9), or AZT glucuronide (UGT2B7).

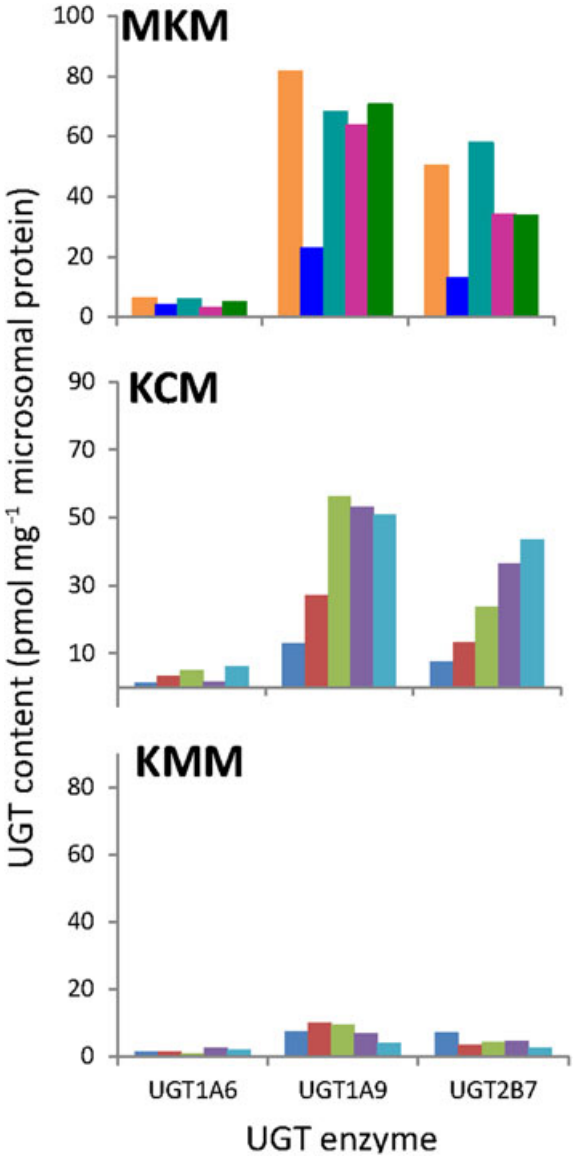

Figure 1

UGT protein concentration (pmol-UGT mg^{-1} microsomal protein) of UGT1A6, UGT1A9 and UGT2B7 of human mixed kidney microsomes (MKM, $n = 5$), kidney cortical microsomes (KCM, $n = 5$) and kidney medullary microsomes (KMM, $n = 5$). Kidney microsomal samples were analyzed at least in duplicate and the values were averaged to obtain a single value for each individual kidney. K2, K7, K9, K10, K11, K12, K13, K14, K15, K16

Cortical and medullary microsomal UGT activities

Similar to MKM, formation of β-E2, TFP or TST glucuronides was not observed using pooled KCM and KMM. Rates of formation (pmol-G min^{-1} mg^{-1} microsomal protein) of DEF (UGT1A6), PRO (UGT1A9) and AZT (UGT2B7) glucuronides by KCM were 1.4-fold, 5.2-fold and 10.5-fold greater, respectively, than for KMM (Table 2). The average cortical : medullary (C : M) ratios of enzyme activity normalized for UGT content were 1.0, 1.1 and 1.8 for UGT 1A6, 1A9 and 2B7, respectively. Comparable enzyme activities were observed for all three

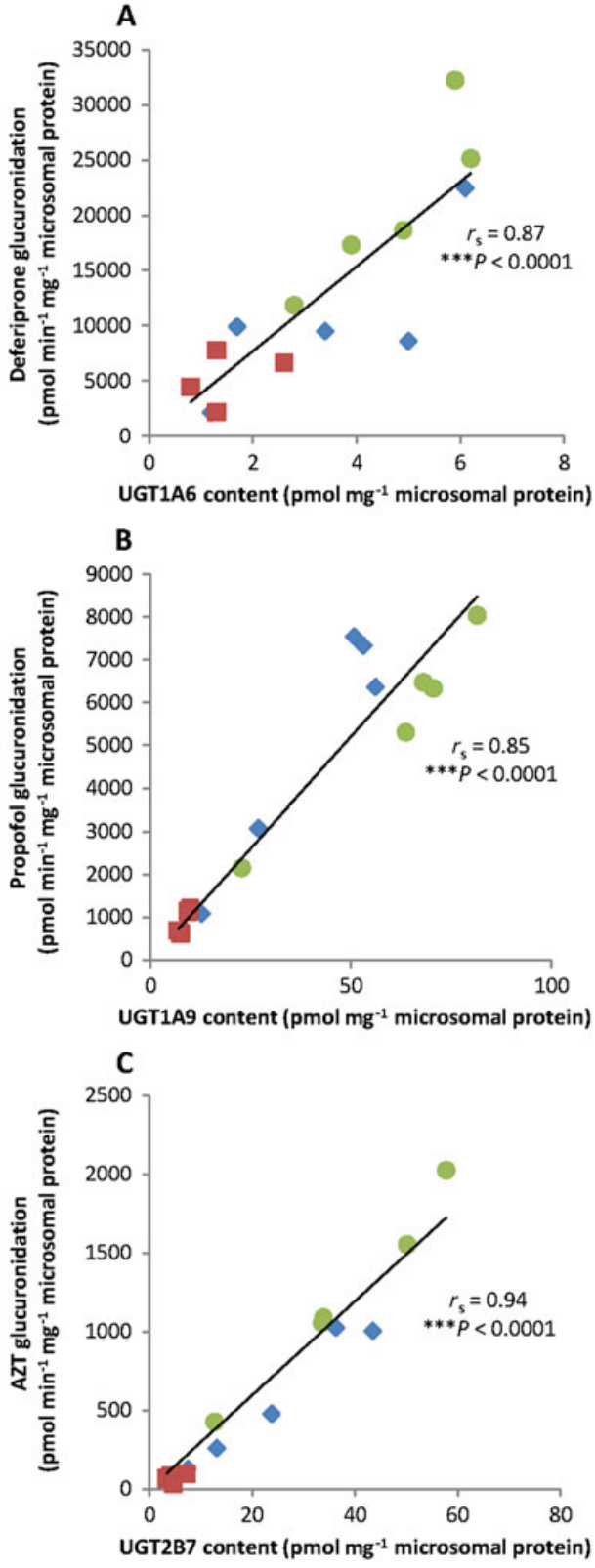

Figure 2

Correlations between (A) deferiprone glucuronidation and UGT1A6 content, (B) propofol glucuronidation and UGT1A9 content and (C) AZT glucuronidation and UGT2B7 content of MKM ●, KCM ◆ and KMM ■. Correlation coefficients r_s were determined using the Spearman rank method.

substrates when using either a pool of KCM or a pool of KMM. The C : M ratios of enzyme activities for the pools of KCM and KMM were 0.9, 0.9 and 1.4 for UGT 1A6, 1A9 and 2B7, respectively (Table 2).

UGT content of human kidney microsomes and UGT 1A9 and UGT2B7 supersomes

In this study the limit of detection for all UGT proteins investigated, except UGT1A8, was <1.0 pmol mg^{-1} protein [20]. UGT 1A6, 1A9 and 2B7 were expressed in all MKM, KCM and KMM samples analyzed (Figure 1). For MKM, the rank order of mean UGT protein content was UGT1A9 (61.3 ± 20.1 pmol mg^{-1}) > UGT2B7 (37.6 ± 17.4 pmol mg^{-1}) > > UGT1A6 (4.7 ± 1.4 pmol mg^{-1}) (Table 1). The content of UGT 1A6, 1A9 and 2B7 protein was greater in KCM, with C : M ratios of 2.7, 6.2 and 7.2, respectively (Table 2). In KCM, the content of UGT1A6 varied approximately 5-fold (range 1.2–6.1 pmol mg^{-1}), 4-fold for UGT1A9 (range 12.8–56.2 pmol mg^{-1}) and 6-fold for UGT2B7 (range 7.4–43.5 pmol mg^{-1}). An approximate 3-fold variation was observed in KMM for UGT1A6 (range 0.8–2.6 pmol mg^{-1}), UGT1A9 (range 3.9–9.9 pmol mg^{-1}) and UGT2B7 (2.5–7.2 pmol mg^{-1}). By contrast, UGT 1A1, 1A3, 1A4, 1A5, 1A7, 1A8, 1A10, 2B4, 2B15 and UGT2B17 were not expressed in MKM, KCM or KMM. UGT2B10 was absent in all MKM samples (K12-K16) and in KCM and KMM for K2, K10 and K11. The UGT1A9 (batch 2 228 592) and UGT2B7 (batch 38 943) contents of Supersomes were 553 pmol mg^{-1} and 1593 pmol mg^{-1}, respectively.

Correlations between glucuronidation activities and UGT protein contents

Rates of glucuronidation of DEF, PRO and AZT by MKM, KCM and KMM were highly correlated with the content of UGT1A6 (r_s = 0.87, $P < 0.0001$), UGT1A9 (r_s = 0.85, $P < 0.0001$) and UGT2B7 (r_s 0.94, $P < 0.0001$), (Figure 2), respectively. Analyses between the contents of UGT enzymes identified significant correlations between the pairs UGT1A6/UGT1A9 (r_s = 0.71, $P < 0.0001$), UGT1A6/UGT2B7 (r_s = 0.76, $P < 0.0001$) and UGT1A9/UGT2B7 (r_s = 0.89, $P < 0.0001$). For individual data refer to Supporting Information Table S2.

PRO and MOR glucuronidation kinetics

Kinetic parameters for PRO glucuronidation by MKM, HLM and UGT1A9 determined in the presence of 2% BSA are shown in Table 3. PRO glucuronidation by all enzyme sources was well described by the Michaelis–Menten equation. Mean K_m values were 17, 9.6 and 9.1 μM for MKM, HLM and UGT1A9, respectively. However, the mean V_{max} value for PRO glucuronidation by MKM was 3.5-fold higher than that for HLM. Hyperbolic kinetics were similarly observed for MOR 3- and 6-glucuronidation by MKM, HLM and recombinant UGT2B7 supplemented with BSA. The mean K_m values for MOR 3- and 6-glucuronidation by the three enzyme sources (+ BSA) ranged from 455 to 602 μM, consistent with previous reports from this laboratory [37, 38]. In contrast to PRO, V_{max} values determined for MOR glucuronidation using HLM were higher than those measured with MKM.

Predicted PRO and MOR CL_{UGT} by kidney and liver

MKM to HLM $CL_{int,u,UGT}$ (μl mg^{-1} min^{-1}) ratios were 2.0 for PRO, and 0.8 and 0.6 for MOR(3-G) and MOR(6-G), respectively (Table 3). Predicted PRO glucuronidation CL_{UGT} by kidney (0.11 ml min^{-1} kg^{-1}) represented 12% of that in liver while scaled total renal MOR glucuronidation CL_{UGT} was 5% of that in liver (Table 3). Extrapolated renal/hepatic PRO CL_{UGT} based on quantification of recombinant UGT1A9 protein was 7% and 6% of the values obtained with MKM and HLM, respectively. Similarly for recombinant UGT2B7 scaled

Table 3

Derived kinetic constants for morphine (MOR) and propofol (PRO) glucuronidation in the presence of 2% (w/v) BSA, scaled $CL_{int,u,UGT}$ g^{-1} of tissue, and predicted *in vivo* glucuronidation clearances (CL_{UGT}) for kidney and liver. The protein sources were pooled mixed human kidney microsomes (MKM), pooled human liver microsomes (HLM), and recombinant human UGT1A9 and UGT2B7

Substrate/Enzyme	K_m* (μM)	V_{max}* (pmol min^{-1} mg^{-1} protein)	$CL_{int,u,UGT}$† (μl min^{-1} mg^{-1} protein)	$CL_{int,u,UGT}$ (ml min^{-1} g^{-1} tissue) Kidney	Liver	Predicted CL_{UGT} (ml min^{-1} kg^{-1}) Kidney	Liver
PRO/MKM	17 ± 0.7	3070 ± 44	181	1.68	–	0.11	–
PRO/HLM	9.6 ± 0.5	880 ± 12.9	91.7	–	2.93	–	0.9
PRO/UGT1 A9	9.1 ± 0.03	997 ± 2.1	110	0.114	0.15	0.008	0.05
MOR(3-G)/MKM	492 ± 2.1	1756 ± 3.4	3.6	0.03	–	0.1	–
MOR(6-G)/MKM	455 ± 10	300 ± 2.0	0.66	0.006	–	0.02	–
MOR(3-G)/HLM	577 ± 10	2544 ± 16	4.4	–	0.14	–	1.9
MOR(6-G)/HLM	533 ± 22	570 ± 9.1	1.1	–	0.04	–	0.48
MOR(3-G)/UGT2B7	602 ± 0.4	835 ± 0.23	1.39	0.0003	0.002	0.0009	0.03
MOR(6-G)/UGT2B7	574 ± 5.8	183 ± 0.7	0.32	0.00007	0.0005	0.0002	0.007

*Parameter ± standard error of parameter fit. †Unbound intrinsic clearance calculated as V_{max}/K_m.3-G = morphine 3-glucuronidation.6-G = morphine 6-glucuronidation.

renal/hepatic MOR glucuronidation CL_{UGT} was 0.9% and 1.6% of CL_{UGT} obtained with MKM and HLM, respectively.

Discussion

The glucuronidation of numerous drugs and other xenobiotics by human kidney has been demonstrated in multiple studies (see Introduction). However, estimates of renal drug metabolic clearance have used either microsomal protein per gram of liver (45 mg g^{-1}, [13]), the yield from rat kidney (6 mg g^{-1}, [9, 41]) or a single report of 12.8 mg g^{-1} [14]. The latter study, which used 5 g of human kidney tissue (unspecified region), reported a 3.8-fold variation in MPPGK (range 4.7–18.2 mg g^{-1}) and a 38% loss of microsomal protein during preparation. Using approximately 1 g of mixed cortical/medullary tissue from five subjects, we determined a mean MPPGK of 9.3 mg g^{-1} (range 6–12 mg g^{-1}). Loss of microsomal protein during preparation was ~34%, comparable with that of Al-Jahdari *et al*. [14], but less than the 47% reported for human liver [29].

The MPPGK determined here is approximately 30% of the value for human liver (32 mg g^{-1}) [16] and therefore estimation of renal drug clearance using hepatic microsomal yield data is clearly inappropriate. A lower microsome yield from kidney in comparison with liver would be anticipated because of the diverse morphology of renal tubule cells that includes well-developed endoplasmic reticulum (ER) in the cortical proximal tubule cells, but sparse ER in tubule cells of the inner zone of the medulla [42]. Additionally, differences in the quantitative distribution of UGTs throughout the human nephron mirror the cortical/medullary gradation of ER [1, 43]. It is unknown if MPPGK changes with ageing, but there were insufficient samples in this study to investigate relationships between MPPGK and the age and gender of the donors. (For individual data refer to Supporting Information Table S2).

The mean rates of DEF, PRO and AZT glucuronidation observed for MKM and paired KCM/KMM were reasonably close in value, 18 999, 6309 and 1183 *vs*. 15 758, 5977 and 647 pmol-G min^{-1} mg^{-1}. The difference in AZT glucuronidation accords with the impact of alternative gene splicing on the activity of UGT2B7 in kidney tissue [44]. Additionally, rates of DEF, PRO and AZT glucuronidation normalized for UGT expression for pooled kidney microsomes are comparable with the rates obtained with the individual kidney microsomes comprising the pool, irrespective of whether the enzyme source was KCM or KMM. Thus, the use of MKM is an appropriate experimental tool for kidney-specific IV–IVE models. Previous studies that have reported the use of kidney microsomes for *in vitro* studies have not specified the anatomic region and hence extrapolated kinetic data may not reflect whole kidney metabolic clearance.

Consistent with other studies reporting lower UGT activity in the medulla than cortex, we found 1.4-, 5- and 11-fold differences between cortex and medulla in the rates of glucuronidation of DEF, PRO and AZT, respectively. The lower activity in medulla equates with the approximate 3-, 6- and 7-fold difference between KCM and KMM in the expression of UGT 1A6, 1A9 and 2B7, respectively. As the region of kidney used for preparation of microsomes impacts on glucuronidation capacity [1], use of KCM will result in an over-estimation and KMM in an under-estimation of CL_{int} via glucuronidation, potentially skewing the role of the kidney in the glucuronidation clearance of drugs and xenobiotics. However, normalizing enzyme activity for UGT expression negates the difference in glucuronidation capacity between KCM and KMM. In addition to anatomic differences in renal glucuronidation, cortical blood flow (4.7 ml g^{-1} tissue min^{-1}) exceeds that of the medulla (2.3 ml g^{-1} tissue min^{-1}) [45]. As noted previously, in the absence of kidney-specific IV–IVE models use of perfusion-limited kinetics and assumptions of the well-stirred model may bias IV–IVE predictions [15].

This study is the first to quantify the UGT protein content of MKM, KCM and KMM and confirms that UGT 1A6, 1A9 and 2B7 are the predominant forms expressed in human kidney [19, 24]. With the exception of UGT 1A6 and 1A9, no quantifiable protein was detected for any of the other UGT1A enzymes investigated. These data support studies reporting either UGT mRNA or UGT protein expression for UGT 1A6 and 1A9 in human kidney [17, 18, 46]. The 13-fold greater abundance of UGT1A9 compared with UGT1A6 supports a greater role for UGT1A9 in the renal metabolism of xeno- and endo-biotics [8]. In contrast, UGT 1A1, 1A3, 1A8 and 1A10 were not detected, which accords with the lack of mRNA expression in kidney [17, 46]. UGT 1A4, 1A5 and 1A7 mRNA expression has been reported [18, 46] but we and Fallon *et al*. [19] found no evidence of the corresponding UGT proteins. Absence of UGT 1A1 and 1A4 protein in renal microsomes is supported by our observation of lack of β-E2 and TFP glucuronidation.

Similar to UGT 1A6 and 1A9, UGT2B7 protein was detected in all MKM, KCM and KMM samples analyzed. On average, UGT2B7 protein expression was approximately half that of UGT1A9, consistent with the lesser contribution of UGT2B7 to overall renal glucuronidation. Although mRNA expression has been reported for UGT2B4 and UGT2B15/17 [46] the corresponding UGT proteins were not detected in this and other studies [19, 24] highlighting the fact that mRNA expression is not predictive at the protein level [47]. Additionally, we did not observe glucuronidation of the UGT2B15/17 'probe' substrate TST by kidney microsomes.

Significant correlations were observed here between UGT 1A6, 1A9 and 2B7 enzyme activity and UGT protein content and between UGT1A6/UGT1A9, UGT1A6/UGT2B7 and UGT1A9/UGT2B7 content. Previous studies have reported a significant correlation between UGT1A6/UGT1A9 expression using HLM [21, 48]. Correlations between UGT 1A6, 1A9 and 2B7 protein content may be explained by common regulatory factors including PXR, CAR, HNF-1α and HNF-4α [49–51]. Additionally, UGT1A9 and UGT2B7 terminate the biological activity of arachidonic acid metabolites and hence are integral to the regulation of renal haemodynamics [7, 8].

Based on experience with the IV–IVE of hepatic drug glucuronidation clearance [30], the results presented here provide an approach for the assessment of the relative contribution of renal and hepatic drug and chemical clearance via glucuronidation from *in vitro* data. As with the IV–IVE of hepatically eliminated drugs the crucial first step is the accurate prediction of *in vitro* CL_{int} (V_{max}/K_m) with MKM as the

enzyme source (or maximal clearance where sigmoidal kinetics are observed). Activation of MKM with alamethicin is necessary to remove the 'latency' associated with microsomal UGTs [34] and, since the predominant UGT enzymes in MKM are UGT 1A9 and 2B7, incubations were performed in the presence of 2% (w/v) BSA to overcome the inhibition of these enzymes by inhibitory long-chain unsaturated acids released from membranes during the course of an incubation [15, 33, 52–54]. However, substrate binding to HLM and BSA must be accounted for in the calculation of K_m (and hence $CL_{int,u,UGT}$). The microsomal $CL_{int,u,UGT}$ may then be scaled to the whole kidney $CL_{int,u,UGT}$ using the MPPGK reported here (i.e. 9.3 mg g^{-1}), which in turn may be scaled to renal glucuronidation clearance. Although the equation for the well-stirred model was used here (and previously by others [15]), its relevance to the prediction of renal drug glucuronidation clearance *in vivo* is yet to be established, especially considering blood flow in the cortex and medulla differ [45].

Following this approach, the extrapolated renal glucuronidation $CL_{int,u,UGT}$ of the UGT1A9 substrate PRO and the UGT2B7 substrate MOR were determined here, along with the predicted renal and hepatic glucuronidation clearances for these drugs. The sum of the extrapolated renal and hepatic PRO glucuronidation clearances was 1.01 ml min^{-1} kg^{-1} or 4.2 l h^{-1} for a 70 kg person. PRO is cleared *in vivo* by both UGT and cytochrome P450 mediated oxidation, predominately UGT1A9 [33] and CYP2B6 [14]. As indicated in Methods the estimated renal clearance via glucuronidation *in vivo* is 57 l h^{-1} [33]. Based on the combined renal and hepatic *in vitro* kinetic data reported here the predicted CL_{UGT} compared with that observed *in vivo* is substantially under-estimated. Of the total PRO glucuronidation clearance predicted from the *in vitro* data, renal glucuronidation accounted for 11% (i.e. 0.11 *vs.* 1.01 ml min^{-1} kg^{-1}). A significant contribution of renal glucuronidation to PRO elimination accords with the observation that extra-hepatic clearance may account for up to 27% of total clearance in patients undergoing liver transplantation, although the separate renal metabolic clearances via glucuronidation and oxidation were not determined [55]. Gill *et al*. [15] recently reported a comparison of the glucuronidation of a number of compounds, including PRO, by HLM and HKM. In contrast to our data (kidney : liver ratio 0.6), these authors noted a higher kidney : liver ratio (1.63) for extrapolated PRO $CL_{int,u,UGT.}$ However, as noted by Gill *et al*. [15], the effect of BSA on *in vitro* $CL_{int,u,UGT}$ with HLM as the enzyme source was considerably lower than the approximate 10-fold increase expected for UGT1A9 substrates and lower than the 11.2-fold increased they observed for HKM. Had the BSA effect been similar to previous reports, recalculating the data reported by Gill *et al*. [15] for the contribution of the kidney to PRO glucuronidation clearance provides a value of 11%, identical to this study. Predicted CL_{UGT} observed here under-estimated the known clearance of PRO by glucuronidation (*viz*. 57 l h^{-1}) by 93%. Similarly the *in vitro* glucuronidation data generated by Gill *et al*. [15] under-estimated known PRO CL_{UGT} by approximately 75%. A number of factors may have contributed to the differences in predicted CL_{UGT} between the two studies. In the study of Gill *et al*. [15] *in vitro* $CL_{int,u,UGT}$ was estimated using the substrate depletion approach compared with the measurement of glucuronide formation here, the anatomical region used for preparation of kidney microsomes was not specified and a value for MPPGK of 12.8 mg g^{-1} was employed. Nevertheless, it is apparent that, despite the determination of MPPGK and knowledge of renal UGT abundance, current IV–IVE approaches under-predict PRO glucuronidation clearance *in vivo*.

Similar to PRO, the predicted renal glucuronidation clearance of the UGT2B7 substrate MOR was also low (5%) compared with the predicted hepatic clearance (0.12 *vs*. 2.38 ml min^{-1} kg^{-1}), which is consistent with the lower expression of UGT2B7 in kidney observed here and by Margaillan *et al*. [24]. The ratio MOR (3-G) : MOR (6-G) was 5 : 1 and 4 : 1 for MKM and HLM, respectively. Similar to PRO, extrapolation of the combined hepatic and renal CL_{UGT} values for MOR 3- and 6-glucuronidation (10.1 l h^{-1}) under-predicted the observed mean *in vivo* glucuronidation clearance (approximately 56.2 l h^{-1} [40]) by 82%. We have observed previously that IV–IVE approaches similarly under-predict the known *in vivo* glucuronidation clearance of the UGT2B7 substrate AZT [34, 54, 56].

The contents of UGT 1A6, 1A9 and 2B7 reported here also potentially allow the prediction of renal/hepatic drug glucuronidation clearance *in vivo* from kinetic data generated using recombinant human UGTs as the enzyme source. We determined *in vitro* $CL_{int,u,UGT}$ values for PRO and MOR glucuronidation by batches of Supersomes expressing UGT1 A9 and UGT2B7, respectively. The specific contents of these UGTs were determined (see Results) and, as anticipated with over-expression, the UGT 1A9 and 2B7 contents of Supersomes (pmol-UGT mg^{-1}) were 10-fold and 43-fold greater than the respective pmol-UGT mg^{-1} of MKM. However, this was not reflected in proportional increases in glucuronidation activities. Compared with the observed total PRO glucuronidation clearance of 57 l h^{-1} the use of recombinant UGT1A9 resulted in a substantial under prediction (0.24 l h^{-1}) although the ratio of the predicted renal to hepatic glucuronidation clearance by UGT1A9 (0.16) was similar to MKM : HLM (0.12). Total MOR glucuronidation clearance (0.17 l h^{-1}) using recombinant UGT2B7 was <1% of the predicted *in vivo* clearance. However, the ratios of MOR(3-G) to MOR(6-G) were similar for all protein sources MKM 6 : 1; HLM 4 : 1 and UGT2B7 5 : 1 (*c.f*. 5.4 *in vivo*) The poor prediction accuracy based on recombinant enzymes may be accounted for by the high levels of inactive protein when UGTs are expressed in insect cells [57].

In conclusion, the cortex has a 5-fold greater abundance of total UGT proteins and hence will have a greater glucuronidation capacity for UGT 1A6, 1A9 and 2B7 substrates than the medulla. This is particularly relevant for UGT1A9 substrates as it is 2.7-fold more abundant in human kidney (61.3 pmol mg^{-1} microsomal protein) than in human liver (approximately 23 pmol mg^{-1}, [20, 48, 58]. Our data support the observation that predicted renal glucuronidation $CL_{int,u,UGT}$ is 2-fold higher in kidney than liver for UGT1A9 substrates [15] and hence $CL_{int,u,UGT}$ should be included in IV–IVE approaches for substrates glucuronidated by UGT1A9. The renal expression of UGT1A6 and UGT2B7 is approximately half that of liver (9.7 and 80.7 pmol mg^{-1}, respectively [20, 58]). Using renal UGT expression data from this

study and liver expression data from Fallon *et al*., [20] the kidney : liver UGT expression ratios for UGT1A6 and UGT2B7 are 0.48 and 0.46. The latter accords well with the kidney : liver scaled $CL_{int,u,UGT}$ ratios of 0.15–0.33 for glucuronidated drugs primarily cleared by UGT2B7 [15] and indicates a greater role normally for UGT2B7 in the hepatic metabolism of xenobiotics. However, in situations impacting on hepatic metabolism (e.g. drug–drug interactions, poor metabolizer phenotype, hepatic transporter defects, hepatic disease) or in the determination of renal metabolite formation or toxicity evaluations, renal glucuronidation by UGT2B7 and indeed UGT1A6 may be an important consideration. Further, we show that the use of recombinant UGT 1A9 and 2B7 proteins is appropriate for determining the contribution and fractional metabolism of substrates but recombinant UGT 1A9 and 2B7 substantially under-predict CL_{UGT}. Clearly further work is still required on the development of relative activity factors, intersystem extrapolation factors and kidney specific IV–IVE models applicable for predicting renal metabolic clearance *in vivo*.

Competing Interests

All authors have completed the Unified Competing Interest Form at http://www.icmje.org/coi_disclosure.pdf (available on request from the corresponding author) and declare no support from any organization for the submitted work, no financial relationships with any organizations that might have an interest in the submitted work in the previous 3 years and no other relationships or activities that could appear to have influenced the submitted work.

KMK had partial grant support from the Faculty of Health Sciences and Flinders Medical Centre Research Foundation, Flinders University; PCS had partial support from the National Institutes of Health (NIH); Instrumentation grant S10, RR024595.

We thank Virginia Papangelis, Flinders Medical Centre/Repatriation General Hospital Tissue Bank Manager for provision of renal tissue and Dr Charles Crespi and Dr Christopher Patten, Corning Gentest for the provision of UGT expressing Supersomes.

Contributors

Participated in research design: KMK, JOM.
Conducted experiments: KMK, SMS, JKF, NC.
Performed data analysis: KMK, SMS, JKF, NC, PCS, JOM.
Wrote or contributed to writing of manuscript: KMK, JKF, JOM.
Final approval of manuscript: KMK, SMS, JKF, NC, PCS, JOM.

References

1 Gaganis P, Miners JO, Brennan JS, Thomas A, Knights KM. Human renal cortical and medullary UDP-glucuronosyltransferases (UGTs): immunohistochemical localization of UGT2B7 and UGT1A enzymes and kinetic characterization of *S*-naproxen glucuronidation. J Pharmacol Exp Ther 2007; 323: 422–30.

2 Bowalgaha K, Elliot DJ, Mackenzie PI, Knights KM, Swedmark S, Miners JO. S-naproxen and desmethylnaproxen glucuronidation by human liver microsomes and recombinant human UDP-glucuronosyltransferases (UGT): role of UGT2B7 in the elimination of naproxen. Br J Clin Pharmacol 2005; 60: 423–33.

3 Rush GF, Hook JB. Characteristics of renal UDP-glucuronosyltransferase. Life Sci 1984; 35: 145–53.

4 Hjelle JT, Hazelton GA, Klaassen CD, Hjelle JJ. Glucuronidation and sulfation in rabbit kidney. J Pharmacol Exp Ther 1986; 236: 150–6.

5 Yue Q, Odar-Cederlof I, Svensson JO, Sawe J. Glucuronidation of morphine in human kidney microsomes. Pharmacol Toxicol 1988; 63: 337–41.

6 Kasichayanula S, Liu X, Pe Benito M, Yao M, Pfister M, LaCreta FP, Griffith Humphreys W, Boulton DW. The influence of kidney function on dapagliflozin exposure, metabolism and pharmacodynamics in healthy subjects and in patients with type 2 diabetes mellitus. Br J Clin Pharmacol 2012; 76: 432–44.

7 Knights KM, Miners JO. Renal UDP-glucuronosyltransferases and the glucuronidation of xenobiotics and endogenous mediators. Drug Metab Rev 2010; 42: 60–70.

8 Knights KM, Rowland A, Miners JO. Renal drug metabolism in humans: the potential for drug-endobiotic interactions involving cytochrome P450 (CYP) and UDP-glucuronosyltransferase (UGT). Br J Clin Pharmacol 2013; 76: 587–602.

9 Bowalgaha K, Miners JO. The glucuronidation of mycophenolic acid by human liver, kidney and jejunum microsomes. Br J Clin Pharmacol 2001; 52: 605–9.

10 McGurk KA, Brierley CH, Burchell B. Drug glucuronidation by human renal UDP-glucuronosyltransferases. Biochem Pharmacol 1998; 55: 1005–12.

11 Mazoit JX, Sandouk P, Scherrmann J-M, Roche A. Extrahepatic metabolism of morphine occurs in humans. Clin Pharmacol Ther 1990; 48: 613–8.

12 Hiraoka H, Yamamoto K, Miyoshi S, Morita T, Nakamura K, Kadoi]Y, Kunimoto F, Horiuchi R. Kidneys contribute to the extrahepatic clearance of propofol in humans, but not lungs and brain. Br J Clin Pharmacol 2005; 60: 176–82.

13 Soars MG, Burchell B, Riley RJ. *In vitro* analysis of human drug glucuronidation and prediction of *in vivo* metabolic clearance. J Pharmacol Exp Ther 2002; 301: 382–90.

14 Al-Jahdari WS, Yamamoto K, Hiraoka H, Nakamura K, Goto F, Horiuchi R. Prediction of total propofol clearance based on enzyme activities in microsomes from human kidney and liver. Eur J Clin Pharmacol 2006; 62: 527–33.

15 Gill KL, Houston JB, Galetin A. Characterization of *in vitro* glucuronidation clearance of a range of drugs in human kidney microsomes: comparison with liver and intestinal glucuronidation and impact of albumin. Drug Metab Dispos 2012; 40: 825–35.

16 Barter ZE, Bayliss MK, Beaune PH, Boobis AR, Carlile DJ, Edwards RJ, Houston JB, Lake BG, Lipscomb JC, Pelkonen OR, Tucker GT, Rostami-Hodjegan A. Scaling factors for the extrapolation of *in vivo* metabolic drug clearance from *in vitro* data: reaching a consensus on values of human microsomal protein and hepatocellularity per gram of liver. Curr Drug Metab 2007; 8: 33–45.

17 Ohno S, Nakajin S. Determination of mRNA expression of human UDP-glucuronosyltransferases and application for localization in

various human tissues by real-time reverse transcriptase-polymerase chain reaction. Drug Metab Dispos 2009; 37: 32–40.

18 Court MH, Zhang X, Ding X, Yee KK, Hesse LM, Finel M. Quantitative distribution of mRNAs encoding the 19 human UDP-glucuronosyltransferase enzymes in 26 adult and 3 fetal tissues. Xenobiotica 2012; 42: 266–77.

19 Fallon JK, Neubert H, Goosen TC, Smith PC. Targeted precise quantification of 12 human recombinant uridine-diphosphate glucuronosyltransferase 1 A and 2B isoforms using nano-ultra-high-performance liquid chromatography/tandem mass spectrometry with selected reaction monitoring. Drug Metab Dispos 2013; 41: 2076–80.

20 Fallon JK, Neubert H, Hyland R, Goosen TC, Smith PC. Targeted quantitative proteomics for the analysis of 14 UGT1As and -2Bs in human liver using nano UPLC–MS/MS with selected reaction monitoring. J Proteome Res 2013; 12: 4402–13.

21 Achour B, Russell MR, Barber J, Rostami-Hodjegan A. Simultaneous quantification of abundance of several cytochrome P450 and uridine 5′-diphospho-glucuronosyltransferase enzymes in human liver microsomes using multiplexed targeted proteomics. Drug Metab Dispos 2014; 42: 500–10.

22 Ohtsuki S, Kawakami H, Inoue T, Nakamura K, Tateno C, Katsukura Y, Obuchi W, Uchida Y, Kamiie J, Horie T, Terasaki T. Validation of uPA/SCID mouse with humanized liver as a model: protein quantification of transporters, cytochromes P450, and UDP-glucuronosyltransferases by LC-MS/MS. Drug Metab Dispos 2014; 42: 1039–43.

23 Harbourt DE, Fallon JK, Ito S, Baba T, Ritter JK, Glish GL, Smith PC. Quantification of human uridine-diphosphate glucuronosyltransferase 1A isoforms in liver, intestine, and kidney using nanobore liquid chromatography–tandem mass spectrometry. Anal Chem 2012; 84: 98–105.

24 Margaillan G, Rouleau M, Fallon JK, Caron P, Villeneuve L, Turcotte V, Smith PC, Joy MS, Guillemette C. Quantitative profiling of human renal UGTs and glucuronidation activity: a comparison of normal and tumoral kidney tissues. Drug Metab Dispos 2015; 43: 611–5.

25 Tsoutsikos P, Miners JO, Stapleton A, Thomas A, Sallustio BC, Knights KM. Evidence that unsaturated fatty acids are potent inhibitors of renal UDP-glucuronosyltransferases (UGT); kinetic studies using human kidney cortical microsomes and recombinant UGT1 A9 and UGT2B7. Biochem Pharmacol 2004; 67: 191–9.

26 Lowry OH, Rosebrough NJ, Farr AL, Randal RJ. Protein measurement with the folin phenol reagent. J Biol Chem 1951; 193: 265–75.

27 Phillips AH, Langdon RG. Hepatic triphosphopyridine nucleotide-cytochrome c reductase: isolation, characterization, and kinetic studies. J Biol Chem 1962; 237: 2652–60.

28 Margoliash E, Frohwirt N. Spectrum of horse-heart cytochrome c. Biochem J 1959; 71: 570–2.

29 Wilson ZE, Rostami-Hodjegan A, Burn JL, Tooley A, Boyle J, Ellis SW, Tucker GT. Inter-individual variability in levels of human microsomal protein and hepatocellularity per gram of liver. Br J Clin Pharmacol 2003; 56: 433–40.

30 Miners JO, Mackenzie PI, Knights KM. The prediction of drug-glucuronidation parameters in humans: UDP-glucuronosyltransferase enzyme-selective substrate and inhibitor probes for reaction phenotyping and *in vitro-in vivo* extrapolation of drug clearance and drug–drug interaction potential. Drug Metab Rev 2010; 42: 196–208.

31 Udomuksorn W, Elliot DJ, Lewis BC, Mackenzie PI, Yoovathaworn K, Miners JO. Influence of mutations associated with Gilbert and Crigler-Najjar type II syndromes on the glucuronidation kinetics of bilirubin and other UDP-glucuronosyltransferase 1 a substrates. Pharmacogenet Genomics 2007; 17: 1017–29.

32 Miners JO, Bowalgaha K, Elliot DJ, Baranczewski P, Knights KM. Characterization of niflumic acid as a selective inhibitor of human liver microsomal UDP-glucuronosyltransferase 1A: application to the reaction phenotyping of acetaminophen glucuronidation. Drug Metab Dispos 2011; 39: 644–52.

33 Rowland A, Knights KM, Mackenzie PI, Miners JO. The "albumin effect" and drug glucuronidation: bovine serum albumin and fatty acid-free human serum albumin enhance the glucuronidation of UDP-glucuronosyltransferase (UGT) 1 A9 substrates but not UGT1A1 and UGT1 A6 activities. Drug Metab Dispos 2008; 36: 1056–62.

34 Boase S, Miners JO. *In vitro–in vivo* correlations for drug eliminated by glucuronidation: investigations with the model substrate zidovudine. Br J Clin Pharmacol 2002; 54: 493–503.

35 Bowalgaha K, Elliot DJ, Mackenzie PI, Knights KM, Miners JO. The glucuronidation of Δ^4 -3-keto C19- and C21-hydroxysteroids by human liver microsomal and recombinant UDP-glucuronosyltransferases (UGTs): 6 α- and 21-hydroxyprogesterone are selective substrates for UGT2B7. Drug Metab Dispos 2007; 35: 363–70.

36 Uchaipichat V, Mackenzie PI, Elliot DJ, Miners JO. Selectivity of substrate (trifluoperazine) and inhibitor (amitriptyline), androsterone, canrenoic acid, hecogenin, phenylbutazone, quinidine, quinine, and sulfinpyrazone) "probes" for human UDP-glucuronosyltransferases. Drug Metab Dispos 2006; 34: 449–56.

37 Uchaipichat V, Raungrut P, Chau N, Janchawee B, Evans AM, Miners JO. Effects of ketamine on human UDP-glucuronosyltransferases *in vitro* predict potential drug–drug interactions from ketamine inhibition of codeine and morphine glucuronidation. Drug Metab Dispos 2011; 39: 1324–8.

38 Chau N, Elliot DJ, Lewis BC, Burns K, Johnston MR, Mackenzie PI, Miners JO. Morphine glucuronidation and glucosidation represent complementary metabolic pathways that are both catalyzed by UDP-glucuronosyltransferase 2B7: kinetic, inhibition, and molecular modeling studies. J Pharmacol Exp Ther 2014; 349: 126–37.

39 Higgins JW, Bao JQ, Ke AB, Manro JR, Fallon JK, Smith PC, Zamek-Gliszczynski MJ. Utility of Oatp1a/1b-knockout and OATP1B1/3-humanized mice in the study of OATP-mediated pharmacokinetics and tissue distribution: case studies with pravastatin, atorvastatin, simvastatin, and carboxydichlorofluorescein. Drug Metab Dispos 2014; 42: 182–92.

40 Milne RW, Nation RL, Somogyi AA. The disposition of morphine and its 3- and 6-glucuronide metabolites in humans and animals, and the importance of the metabolites to the pharmacological effects of morphine. Drug Metab Rev 1996; 28: 345–472.

41 Aitio A, Vainio H. UDP-glucuronosyltransferase and mixed function oxidase activity in microsomes prepared by differential centrifugation and calcium aggregation. Acta Pharmacol Toxicol 1975; 39: 555–61.

42 Bohman S-V. The ultrastructure of the renal medulla and interstitial cells. In: The renal papilla and hypertension, eds Mandal AK, Bohman S-V. New York: Springer Science + Business Media, 1980; 7–33.

43 Bellemare J, Rouleau M, Harvey M, Popa I, Pelletier G, Tetu B, Guillemette C. Immunohistochemical expression of conjugating UGT1A-derived isoforms in normal and tumoral drug-metabolizing tissues in humans. J Pathol 2011; 223: 425–35.

44 Menard V, Levesque E, Chen S, Eap O, Joy MS, Ekstrom L, Rane A, Guillemette C. Expression of UGT2B7 is driven by two mutually exclusive promoters and alternative splicing in human tissues: changes from prenatal life to adulthood and in kidney cancer. Pharmacogenet Genomics 2013; 23: 684–96.

45 Damkjaer M, Vafee M, Moller ML, Braad PE, Petersen H, Hoilund-Carlsen PF, Bie P. Renal cortical and medullary blood flow responses to altered NO availability in humans. Am J Physiol Regul Integr Comp Physiol 2010; 299: R1449–55.

46 Nakamura A, Nakajima M, Yamanaka H, Fujiwara R, Yokoi T. Expression of UGT1A and UGT2B mRNA in human normal tissues and various cell lines. Drug Metab Dispos 2008; 36: 1461–4.

47 Guo Y, Xiao P, Lei S, Deng F, Xiao GG, Liu Y, Chen X, Li L, Wu S, Chen Y, Jiang H, Tan L, Xie J, Zhu X, Liang S, Deng H. How is mRNA expression predictive for protein expression? A correlation study on human circulating monocytes. Acta Biochim Biophys Sin 2008; 40: 426–36.

48 Margaillan G, Rouleau M, Klein K, Fallon JK, Caron P, Villeneuve L, Smith PC, Zanger UM, Guillemette C. Multiplexed targeted quantitative proteomics predicts hepatic glucuronidation potential. Drug Metab Dispos 2015; 43: 1331–5.

49 Aueviriyavit S, Furihata T, Morimoto K, Kobayashi K, Chiba K. Hepatocyte nuclear factor 1 alpha and 4 alpha are factors involved in interindividual variability in the expression of UGT1A6 and UGT1A9 but not UGT1A1, UGT1A3 and UGT1A4 mRNA in human livers. Drug Metab Pharmacokinet 2007; 22: 391–8.

50 Foti RS, Fisher MB. UDP-glucuronosyltransferases: Pharmacogenetics, functional characterization, and clinical relevance. In: Encyclopedia of Drug Metabolism and Interactions, eds Lyubimov A, Rodrigues AD, Sinz M. New Jersey: John Wiley & Sons, 2012; 1–71.

51 Hui DG, Meech R, McKinnon RA, Mackenzie PI. Transcriptional regulation of UDP-glucuronosyltransferase genes. Drug Metab Rev 2014; 46: 421–58.

52 Rowland A, Gaganis P, Elliot DJ, Mackenzie PI, Knights KM, Miners JO. Binding of inhibitory fatty acids is responsible for the enhancement of UDP-glucuronosyltransferase 2B7 activity by albumin: implications for *in vitro-in vivo* extrapolation. J Pharmacol Exp Ther 2007; 321: 137–47.

53 Manevski N, Morcolo PS, Yli-Kauhaluoma J, Finel M. Bovine serum albumin decreases K_m values of human UDP-glucuronosyltransferases 1A9 and 2B7 and increases V_{max} values of UGT1A9. Drug Metab Dispos 2011; 39: 2117–29.

54 Walsky RL, Bauman JN, Bourcier K, Giddens G, Lapham K, Negahban A, Ryder TF, Obach RS, Hyland R, Goosen TC. Optimized assays for human UDP-glucuronosyltransferase (UGT) activities: altered alamethicin concentration and utility to screen for UGT inhibitors. Drug Metab Dispos 2012; 40: 1051–65.

55 Takizawa D, Hiraoka H, Nakamura K, Yamamoto K, Horiuchi R. Propofol concentrations during the anhepatic phase of living-related donor liver transplantation. Clin Pharmacol Ther 2004; 76: 648–9.

56 Kilford PJ, Stringer R, Sohal B, Houston JB, Galetin A. Prediction of drug clearance by glucuronidation from *in vitro* data: use of combined cytochrome P450 and UDP-glucuronosyltransferase cofactors in alamethicin-activated human liver microsomes. Drug Metab Dispos 2009; 37: 82–9.

57 Zhang H, Patana A-S, Mackenzie PI, Ikushiro S, Goldman A, Finel M. Human UDP-glucuronosyltransferase expression in insect cells: ratio of active to inactive recombinant proteins and the effects of a C-terminal his-tag on glucuronidation kinetics. Drug Metab Dispos 2012; 40: 1935–44.

58 Zientek MA, Youdim K. Reaction phenotyping: advances in the experimental strategies used to characterize the contribution of drug metabolizing enzymes. Drug Metab Dispos 2015; 43: 163–81.

Supporting Information

Additional Supporting Information may be found in the online version of this article at the publisher's web-site:

http://onlinelibrary.wiley.com/doi/10.1111/bcp.12889/suppinfo.

Table S1 Human kidney donor details and drug history.
Table S2 UGT protein concentration (pmol-UGT mg^{-1} microsomal protein) of UGT1A6, UGT1A9 and UGT2B7 of human mixed kidney microsomes (MKM, n = 5), kidney cortical microsomes (KCM, n = 5) and kidney medullary microsomes (KMM, n = 5) and microsomal protein per gram of kidney (mg g^{-1}, MPPGK) of MKM. Data are tabulated as the means of duplicate (UGT 1A6, 1A9 and 2B7) or triplicate (MPPGK) determinations